

Motional frequency shifts of trapped ions in the Lamb-Dicke regime

I. Lizuain* and J. G. Muga†

Departamento de Química-Física, Universidad del País Vasco, Apdo. 644, Bilbao, Spain

J. Eschner‡

ICFO, Institut de Ciències Fotòniques, 08860 Castelldefels, Barcelona, Spain

First order Doppler effects are usually ignored in laser driven trapped ions when the recoil frequency is much smaller than the trapping frequency (Lamb-Dicke regime). This means that the central, carrier excitation band is supposed to be unaffected by vibronic transitions in which the vibrational number changes. While this is strictly true in the Lamb-Dicke limit (infinitely tight confinement), the vibronic transitions do play a role in the Lamb-Dicke regime. In this paper we quantify the asymptotic behaviour of their effect with respect to the Lamb-Dicke parameter. In particular, we give analytical expressions for the frequency shift, “pulling” or “pushing”, produced in the carrier absorption band by the vibronic transitions both for Rabi and Ramsey schemes. This shift is shown to be independent of the initial vibrational state.

PACS numbers: 03.75.Dg, 06.30.Ft, 39.20.+q, 42.50.Vk

I. INTRODUCTION

There is currently much interest in laser cooled trapped ions because of metrological applications as frequency standards, high precision spectroscopy, or the prospects of realizing quantum information processing [1]. The absorption spectrum of a harmonically trapped (two-level) ion consists of a carrier band at the transition frequency ω_0 and first order Doppler effect generated sidebands, equally spaced by the trap frequency ω_T , see Fig. 1. The excitation probability of a given sideband, and thus its intensity, depends critically on the so-called Lamb-Dicke (LD) parameter $\eta = [\hbar k_L^2 / (2m\omega_T)]^{1/2}$, with k_L being the driving laser wave number. If the LD regime is assumed ($\eta \ll 1$), the intensity of the k th red or blue sideband scales with η^k [1, 2, 3], $k = 1, 2, 3, \dots$, so the number of visible sidebands diminishes by decreasing η . It is then usually argued that in the LD regime the absorption at the carrier frequency is free from first order Doppler effect [3, 4, 5]. Of course this is only exact in the strict Lamb-Dicke limit, $\eta = 0$, and for high precision spectroscopy, metrology, or quantum information applications, it is important to quantify the effect of the sideband transitions in the carrier peak, in other words, the asymptotic behaviour, as $\eta \sim 0$, of the frequency shift of the carrier peak contaminated by vibronic, also called sideband, transitions in which the vibrational state changes.¹ The inverse effect, in which the sideband is shifted by a non-resonant coupling to the carrier, has been previously studied in the field of trapped-ion based quantum

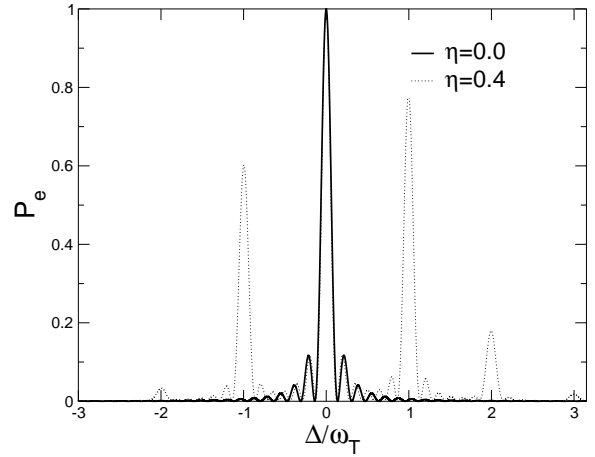


FIG. 1: Excited state probability of a trapped ion after a π -pulse has been applied. The ion is initially in the $|g, 2\rangle$ state.

computers [6, 7]. To get insight and the reference of analytical results, we shall examine a simplified one dimensional model neglecting decay from the excited state (resolved sideband regime [8]). The shift dependence on the various parameters (duration of the laser pulses, Rabi frequency Ω_R , ω_T) will be explicitly obtained making use of a dressed state picture and a perturbation theory with respect to η . The cases of Rabi and Ramsey excitations will be examined separately since they may be quite different quantitatively and have different applications as we shall see.

A. Notation and Hamiltonian

We consider a two level ion, with ground ($|g\rangle$) and excited ($|e\rangle$) states and transition frequency $\omega_0 = \omega_e - \omega_g$, which is harmonically trapped and illuminated by a

*Email address: ion.lizuain@ehu.es

†Email address: jg.muga@ehu.es

‡Email address: juergen.eschner@icfo.es

¹ Even though several transitions contribute to a given peak, it is named according to the dominant transition: thus we have a carrier peak or k -th sideband peaks.

monochromatic laser of frequency ω_L . In a frame rotating with the laser frequency, i.e., in a laser adapted interaction picture defined by $H_0 = \frac{1}{2}\hbar\omega_L\sigma_z$, and in the usual (optical) Rotating Wave Approximation (RWA), the ion is described by the time independent Hamiltonian [9, 10]

$$H = \hbar\omega_T (a^\dagger a + 1/2) - \frac{\hbar\Delta}{2}\sigma_z + \frac{\hbar\Omega_R}{2} [e^{i\eta(a+a^\dagger)}\sigma_+ + h.c.], \quad (1)$$

where $\Delta = \omega_L - \omega_0$ is the frequency difference between the laser and the internal transition (detuning), $\sigma_z = |e\rangle\langle e| - |g\rangle\langle g|$, $\sigma_+ = |e\rangle\langle g|$, $\sigma_- = |g\rangle\langle e|$, and a, a^\dagger are annihilation and creation operators for the vibrational quanta.

Let us denote by $|g, n\rangle$ ($|e, n\rangle$) the state of the ion in the ground (excited) internal state and in the n^{th} motional level of the harmonic oscillator. In general the Hamiltonian (1) will couple internal and motional states. The $\{|g, n\rangle, |e, n\rangle\}$ states form the ‘‘bare’’ basis of the system, i.e., the eigenstates of the bare hamiltonian $H_B = H(\Omega_R = 0)$. The energy levels corresponding to the bare states are given by

$$\begin{aligned} \epsilon_{g,n} &= E_n + \frac{\hbar\Delta}{2}, \\ \epsilon_{e,n} &= E_n - \frac{\hbar\Delta}{2}, \end{aligned} \quad (2)$$

with $E_n = \hbar\omega_T (n + 1/2)$ being the energies of the harmonic oscillator. These bare energy levels are plotted in Fig. 2 (dotted lines) [9, 10] as a function of the detuning. They are degenerate when $\Delta = \pm k\omega_T$, $k = 0, 1, 2, \dots$, but the degeneracies are removed and become avoided crossings when the laser is turned on, see Fig. 2 (solid lines). At these avoided crossings transitions will occur between the involved (bare) states, which are nothing but the mentioned carrier ($k = 0$) and sideband ($k \geq 1$) transitions [1]. The splitting at each crossing gives the coupling strength of a given transition [10], and the dynamics of the system is then governed essentially by the reduced 2-dimensional Hamiltonian of the involved levels.

Apart from these resonant transitions, off-resonant effects will also take place since, strictly speaking, the system is not 2-dimensional. In particular, near the atomic transition resonance ($\Delta \sim 0$), there will be a finite probability, although small, of exciting higher order sidebands, which tends to zero in the LD limit ($\eta \rightarrow 0$). In this paper we study how these off-resonant effects behave within the LD regime, when η is made asymptotically small but not zero. In particular, we study how these effects affect the excited (internal) state probability, shifting the position of the central resonance, which is crucial in fields such as atom interferometry [11] or atomic clocks with single trapped ions [12], where tiny deviations from the Doppler free form of the probability distribution could affect the accuracy of the measurements. Possible effects for state preparation in quantum information processing are also studied.

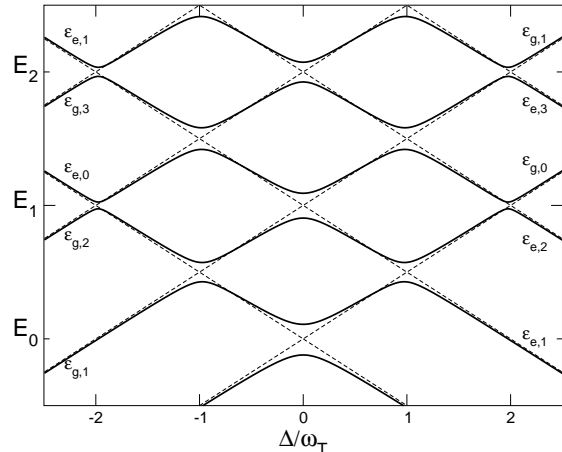


FIG. 2: Bare ($\Omega_R = 0$, dashed line) and dressed ($\Omega_R/\omega_T = 0.3$, solid line) energy levels (in arbitrary units) as a function of the laser detuning. A not to small LD parameter $\eta = 0.4$ has been intentionally chosen in order to highlight the higher order avoided crossings.

II. FREQUENCY SHIFT

In precision spectroscopy experiments, the measured quantity is usually the excited (internal) state probability P_e , regardless of the vibrational quantum number n . If a general state of the trapped ion has the form

$$|\psi(t)\rangle = \sum_{n=0}^{\infty} [g_n(t)|g, n\rangle + e_n(t)|e, n\rangle], \quad (3)$$

the excited state probability P_e will be given by

$$P_e = \text{tr}(|\psi\rangle\langle\psi|e\rangle\langle e|) = \sum_{n=0}^{\infty} P_{e,n}, \quad (4)$$

where $P_{e,n} = |e_n(t)|^2$ is the probability of finding the $|e, n\rangle$ state. In principle, the sum is over the infinite number of available vibrational quantum states, but it can be simplified if the LD regime is assumed. In this regime the extension of the ion’s wavefunction is much smaller than the driving laser wavelength, $\eta \ll 1$, and it is possible to expand the Hamiltonian (1) in powers of η ,

$$H_{LD} = \hbar\omega_T (a^\dagger a + 1/2) - \frac{\hbar\Delta}{2}\sigma_z + \frac{\hbar\Omega_R}{2} [(1 + i\eta a + i\eta a^\dagger)\sigma_+ + h.c.], \quad (5)$$

which only couples, in first order, consecutive motional states. Then, if the ion is initially in the vibrational level n_0 , only consecutive levels $n_0 \pm 1$ will be coupled in a first order approximation. In other words, only carrier,

first blue and first red sidebands will give appreciable contributions to $P_e(\Delta \sim 0)$. It is thus possible to keep only the n_0 and $n_0 \pm 1$ vibrational states and restrict our study to the 6-dimensional subspace spanned by the $\{|g, n_0\rangle, |e, n_0\rangle, |g, n_0 \pm 1\rangle, |e, n_0 \pm 1\rangle\}$ bare states. The excited state probability (4) can then be approximated by

$$P_e \approx P_{e, n_0-1} + P_{e, n_0} + P_{e, n_0+1} \quad (6)$$

in the LD regime. For all numerical cases examined, we have checked that adding further vibrational levels and using the Hamiltonian (1) leads to indistinguishable results with respect to the six-state model if the LD condition is satisfied.

For an infinitely narrow trap ($\eta \rightarrow 0$), only carrier transitions are driven (i.e., transitions in which the vibrational quantum number is not changed) and the central (carrier) peak of the excited state probability is exactly at atomic resonance, i.e., at $\Delta = 0$. The generation of blue and red sidebands will affect this distribution shifting the central maximum by δ , where δ is the detuning that satisfies the maximum condition

$$\left. \frac{dP_e}{d\Delta} \right|_{\Delta=\delta} \approx \left. \frac{d}{d\Delta} (P_{e, n_0-1} + P_{e, n_0} + P_{e, n_0+1}) \right|_{\Delta=\delta} = 0 \quad (7)$$

and defines the ‘‘frequency shift’’ in the following sections. This frequency shift can be understood as the error in determining the center of the resonance, i.e., the position of the maximum excitation. It will be shown that the position of this maximum, rather than coinciding with the line center, varies periodically with the trap frequency ω_T when the sidebands are taken into account.

In the following sections this shift will be calculated in different excitation schemes, such as Rabi excitation (a single pulse, which is used in atomic clocks as well as quantum logic applications); and Ramsey interferometry (two pulses applied in atomic clocks and frequency standards).

III. SINGLE PULSE (RABI) EXCITATION

If an ion is prepared in $|\psi(t_i)\rangle$ at an initial time t_i , the state of the system at a later time t_f will be given by

$$\begin{aligned} |\psi(t_f)\rangle &= e^{-iH(t_f-t_i)/\hbar} |\psi(t_i)\rangle \\ &= \sum_{\alpha} e^{-i\epsilon_{\alpha}(t_f-t_i)/\hbar} |\epsilon_{\alpha}\rangle \langle \epsilon_{\alpha} | \psi(t_i)\rangle, \end{aligned} \quad (8)$$

where $|\epsilon_{\alpha}\rangle$ (ϵ_{α}) are the α^{th} dressed states (energies) of the system, i.e., eigenstates (eigenenergies) of H . We will consider first the case where a trapped ion is prepared in a given state $|g, n_0\rangle$ at time $t_i = 0$ and illuminated by a single Rabi laser pulse for a time τ .

The partial probabilities are easily obtained by projecting the $|e, n\rangle$ state on the state of the system at time

τ ,

$$\begin{aligned} P_{e, n} &= |\langle e, n | \psi(\tau) \rangle|^2 \\ &= \left| \sum_{\alpha} e^{-i\epsilon_{\alpha}\tau/\hbar} \langle e, n | \epsilon_{\alpha} \rangle \langle \epsilon_{\alpha} | g, n_0 \rangle \right|^2, \end{aligned} \quad (9)$$

see an example in Fig. 1. For an infinitely narrow trap ($\eta = 0$), $P_e(\Delta)$ is the well known Rabi pattern (solid line of Fig. 1). For non-zero LD parameters, sidebands are generated at integer multiples of the trap frequency ω_T , (dotted line in Fig. 1). To obtain analytical expressions for these partial probabilities we shall follow the perturbative approach introduced in [10].

A. Perturbative analysis: ‘‘Semidressed’’ states.

The perturbative approach in [10] consists on dividing the Hamiltonian in Eq. (5) as

$$H_{LD} = H_{SD} + V(\eta), \quad (10)$$

with

$$\begin{aligned} H_{SD} &= \hbar\omega_T (a^{\dagger}a + 1/2) - \frac{\hbar\Delta}{2}\sigma_z + \frac{\hbar\Omega_R}{2}(\sigma_+ + \sigma_-), \\ V(\eta) &= \frac{\hbar\Omega_R\eta}{2} [i(a + a^{\dagger})\sigma_+ + h.c.], \end{aligned} \quad (11)$$

where H_{SD} is a ‘‘semi-dressed’’ Hamiltonian, which describes the trapped ion coupled to a laser field, but does not account for the coupling between different vibrational levels. This coupling is described by the term $V(\eta)$. Note that H_{LD} reduces to H_{SD} in the LD limit ($\eta \rightarrow 0$), and $V(\eta)$ is a small perturbation of H_{SD} in the LD regime, $\eta \ll 1$.

Within this perturbative scheme, dressed states and energies of H_{LD} are obtained up to leading order in the LD parameter η in our 6-dimensional sub-space, see Appendix A.

B. Excited state probability

With the expressions of the dressed energies (A4) and dressed states (A5) of H_{LD} , one finds, after some lengthy algebra from Eq. (9), that the probability of finding the ion in the internal excited state after a laser pulse of duration τ is given, for the three relevant motional levels,

by

$$\begin{aligned}
P_{e,n_0-1} &= n_0 \frac{\eta^2 \Omega_R^2}{\Omega^2 (\omega_T^2 - \Omega^2)^2} \\
&\times \left[(\Delta - \omega_T) \Omega \cos \frac{\Omega\tau}{2} \sin \frac{\omega_T\tau}{2} \right. \\
&\left. + (\Omega^2 - \Delta\omega_T) \sin \frac{\Omega\tau}{2} \cos \frac{\omega_T\tau}{2} \right]^2, \\
P_{e,n_0} &= \left(\frac{\Omega_R}{\Omega} \right)^2 \sin^2 \frac{\Omega\tau}{2} + \frac{\eta^2 \Omega_R^4}{4\Omega^2} (2n_0 + 1) \sin \frac{\Omega\tau}{2} \\
&\times \left[\frac{\sin(\omega_T\tau - \Omega\tau/2)}{(\omega_T - \Omega)^2} - \frac{\sin(\omega_T\tau + \Omega\tau/2)}{(\omega_T + \Omega)^2} \right], \\
P_{e,n_0+1} &= (n_0 + 1) \frac{\eta^2 \Omega_R^2}{\Omega^2 (\omega_T^2 - \Omega^2)^2} \\
&\times \left[(\Delta + \omega_T) \Omega \cos \frac{\Omega\tau}{2} \sin \frac{\omega_T\tau}{2} \right. \\
&\left. - (\Omega^2 + \Delta\omega_T) \sin \frac{\Omega\tau}{2} \cos \frac{\omega_T\tau}{2} \right]^2, \quad (12)
\end{aligned}$$

where $\Omega \equiv \sqrt{\Omega_R^2 + \Delta^2}$ is the effective (detuning dependent) Rabi frequency.

These probabilities are different from the ones obtained if counter rotating terms in Hamiltonian (5) are neglected after applying a motional or vibrational RWA. In this case, instead of a six-dimensional model, three 2-dimensional models are solved [1], to yield

$$P_{e,n+k} = \left| \frac{\Omega_{n,n+k}}{f_n^k} \right|^2 \sin^2 \frac{f_n^k \tau}{2}, \quad (13)$$

where $\Omega_{n,n+k} = \Omega_R \langle n | e^{i\eta(a+a^\dagger)} | n+k \rangle$ and

$$f_n^k = \sqrt{(\Delta - k\omega_T)^2 + \Omega_{n,n+k}^2}. \quad (14)$$

These simplified expressions for the excited state probabilities give quite different frequency shifts as discussed later, and do not add to one exactly at one particular value of the detuning.

C. Rabi frequency shift

We are interested in the behaviour of P_e near resonance, i.e., $\Delta \sim 0$. If only leading terms in Δ are kept and the maximum condition (7) is applied to the probabilities in Eq. (12), it is found that for a weak laser (“weak” meaning here that $\alpha \equiv \Omega_R/\omega_T \ll 1$), the frequency shift oscillates with the trap frequency ω_T as

$$\delta(\tau) \approx \Omega_R \eta^2 \alpha^2 f(\Omega_R \tau) \sin \omega_T \tau, \quad (15)$$

with $f(\xi)$ being the function

$$f(\xi) = \frac{\sin \xi}{\xi \sin \xi - 4 \sin^2 \frac{\xi}{2}}. \quad (16)$$

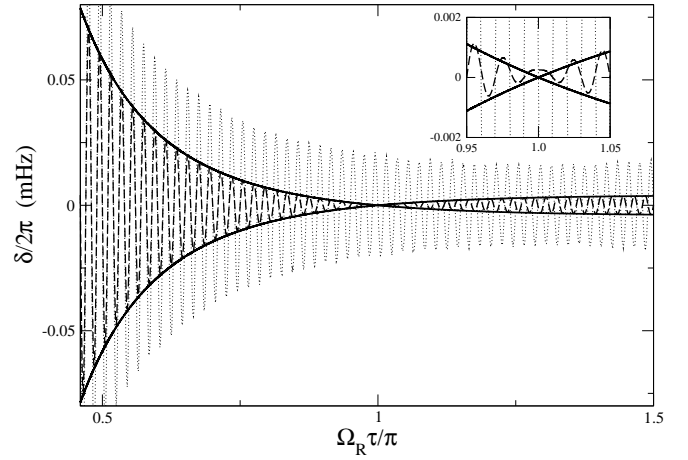


FIG. 3: Exact (numerical) (dashed line) frequency shift after a Rabi pulse of duration τ with a fixed Rabi frequency of $\Omega_R = 2\pi \times 100\text{Hz}$ and $\eta = 0.05$. The solid lines represent approximate upper and lower bounds for the shift and the dotted one the shift obtained if the vibrational RWA is applied (using Eq. (13) for the probabilities). Usual Paul (RF) traps have motional frequencies of a few MHz, but in this plot a trap frequency of $\omega_T = 2\pi \times 10\text{kHz}$ has been considered in order to distinguish the fast oscillations. A zoom around the π -pulse is shown in the inset.

The exact (numerical) frequency shift δ is plotted in Fig. 3 (dashed line) as a function of the pulse duration time. The numerical calculations have been performed with the full Hamiltonian (1), i. e., to all orders in the LD expansion, and with a large basis of bare states (more than 6). Here, and in all remaining figures, the numerical results or the analytical approximation obtained in the LD regime are indistinguishable.

The upper and lower approximate bounds for the frequency shift (solid lines in Fig. 3) are obtained at the bounds of the fast oscillating term, i.e., replacing $\sin \omega_T \tau$ by ± 1 in Eq. (15),

$$\delta(\tau) \approx \Omega_R \eta^2 \alpha^2 f(\Omega_R \tau). \quad (17)$$

If the applied pulse is a π -pulse ($\tau_\pi = \pi/\Omega_R$), the leading order contribution to the shift (15) vanishes and the next order in α has to be considered. Under the π -pulse condition there is some robustness against the shift error, reducing the frequency shift to a pulling effect (i.e., a positive shift),

$$\delta(\tau_\pi) \approx \Omega_R \eta^2 \alpha^3 \cos^2 \frac{\omega_T \tau_\pi}{2}, \quad (18)$$

which is not zero (see inset in Fig. 3) except for the values of Ω_R that make the argument of the cosine a multiple of $\pi/2$.

Remarkably, the general frequency shift (15) is independent of the initial vibrational quantum number n_0 . This follows from the fact that the probability for the first red sideband is proportional to the initial motional

Ion	$\omega_T/2\pi$	η	$\Omega_R/2\pi$ (Hz)	$\delta/2\pi$ (Hz)	Reference
$^{40}\text{Ca}^+$ (729nm)	1MHz	0.095	10 – 100	$10^{-12} - 10^{-9}$	[13]
$^{199}\text{Hg}^+$ (282nm)	few MHz	0.035	10 – 20	$10^{-14} - 10^{-13}$	[14, 15]
$^{88}\text{Sr}^+$ (674nm)	2.5MHz	0.042	250 – 500	$10^{-9} - 10^{-8}$	[16]

TABLE I: Rabi one pulse excitation (clocks and frequency standards): for $^{199}\text{Hg}^+$, η and δ have been calculated with $\omega_T/2\pi = 10\text{MHz}$.

Ion	$\omega_T/2\pi$	η	$\Omega_R/2\pi$ (kHz)	$\delta/2\pi$ (Hz)	Reference
Ba^+ (650nm)	50kHz	0.26	1.5 – 15	$10^{-1} - 10^2$	[17]
$^{40}\text{Ca}^+$ (729nm)	2MHz	0.03	5	10^{-5}	[18]

TABLE II: Rabi one pulse excitation: Quantum information and quantum logic.

state n_0 while the first blue sideband is proportional to $n_0 + 1$, see Eqs. (12). When the maximum condition (7) is applied, the n_0 's are cancelled. Moreover, the result is identical to the shift when the ion is initially in the lowest vibrational state. In this case, the frequency shift is just due to the first blue sideband (no red sidebands exist) but $n_0 = 0$. This particular case can be solved exactly in a 4-state model, without a perturbative approach, giving the same results, see the Appendix B.

Note also that if the vibrational RWA is applied and the simplified expressions for the probabilities of the ex-

cited states (13) are used to compute the frequency shift, quite different results are obtained (dotted line in Fig. 3), with particularly high relative errors near the π -pulse condition.

In quantum information applications, the parameters α and Ω_R are usually higher than in frequency standards since the speed of the operations is of importance, so that the shift of the carrier peak may be much larger. We have collected some typical numerical values in Tables I and II.

D. Fidelity for a $\pi/2$ -pulse

The oscillations of the carrier peak shift with respect to $\omega_T\tau$, Eq. (15), may affect other observables as well. As an example we find similar oscillations in the context of quantum state preparation. When applying a resonant $\pi/2$ -pulse to a trapped ion initially in the ground state the internal state obtained for $\eta = 0$ is

$$|\psi_{id}\rangle = \frac{1}{\sqrt{2}} (|g\rangle + i|e\rangle). \quad (19)$$

The contamination due to the higher order sidebands for non-zero η will make the real internal state differ from this ideal state.

We now define the fidelity \mathcal{F} as the probability of detecting the ideal state (19),

$$\mathcal{F} = P_{id} = \text{tr} [|\psi(\tau)\rangle\langle\psi(\tau)|\psi_{id}\rangle\langle\psi_{id}|] \quad (20)$$

$$= \frac{1}{2} \sum_{n=0}^{\infty} |g_n(\tau) - ie_n(\tau)|^2, \quad (21)$$

see Eq. (3), where the sum is in principle over the infinite number of vibrational levels. It is plotted in Fig. 4 as a function of $\alpha = \Omega_R/\omega_T$. The fidelity is unity in the “ideal” $\eta = 0$ case but smaller otherwise. This fidelity oscillates also with the trap frequency, as it is observed in Fig. 4. If a $\pi/2$ -pulse is considered, we may rewrite the expression for the shift (15) as

$$\delta \propto \sin \omega_T\tau = \sin \frac{\Omega_R\tau}{\alpha} = \sin \frac{\pi}{2\alpha}. \quad (22)$$

The maxima of the $\sin \frac{\pi}{2\alpha}$ function are marked with circles in the abscissa.

IV. RAMSEY INTERFEROMETRY

We may also calculate the frequency shift due to generation of higher order sidebands in a Ramsey scheme of two separated laser fields [19]. In these experiments with trapped ions, one ion prepared in the $|g, n_0\rangle$ state is illuminated with two $\pi/2$ -pulses ($\tau_{\pi/2} = \pi/2\Omega_R$) separated

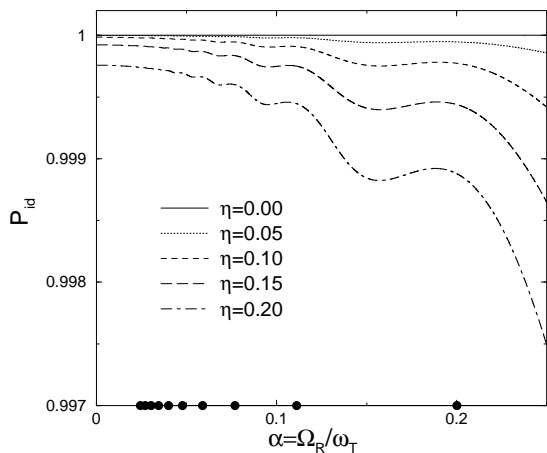


FIG. 4: Probability of detecting the ideal state $|\psi_{id}\rangle$ as a function of $\alpha = \Omega_R/\omega_T$ for different LD parameters. The value of Ω_{RT} is fixed by the (resonant $\Delta = 0$) $\pi/2$ -pulse condition. The circles shown in the abscissa correspond to the maxima of the $\sin \frac{\pi}{2}\alpha$ function, i. e., $\alpha = \frac{1}{4n+1}$ with $n = 0, 1, 2, \dots$

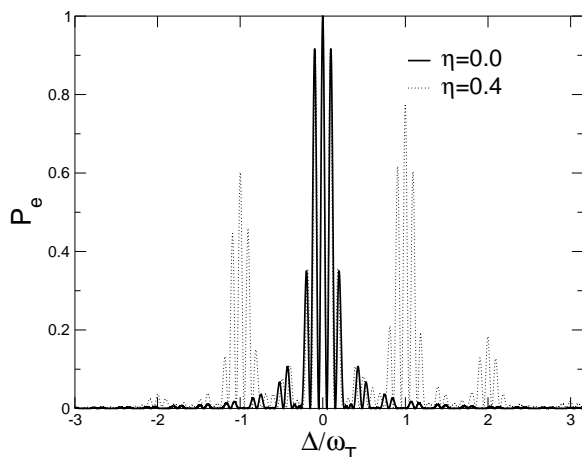


FIG. 5: Ramsey interference pattern for a non interaction time $T = 2\tau$ and for different LD parameters. An ion initially in the $|g, 2\rangle$ state has been considered.

by a non-interaction or intermediate time T . The state of the system at a time $2\tau_{\pi/2} + T$, after the two laser pulses, in the same laser-adapted interaction picture used before ($H_0 = \frac{1}{2}\hbar\omega_L\sigma_z$) is given by

$$|\psi(2\tau_{\pi/2} + T)\rangle = e^{-iH\tau_{\pi/2}/\hbar} e^{-iH_B T/\hbar} e^{-iH\tau_{\pi/2}/\hbar} |g, n_0\rangle, \quad (23)$$

where $H_B = H(\Omega_R = 0)$ is the bare Hamiltonian governing the dynamics of the system in the intermediate region. A simple generalization of Eq. (9) for two separated laser pulses, gives the probability for the different

transitions,

$$P_{e,n} = \left| \sum_{\beta} \sum_{j,k} \sum_{\alpha} e^{-i\epsilon_{\beta}\tau_{\pi/2}/\hbar} e^{-i\epsilon_{j,k}T/\hbar} e^{-i\epsilon_{\alpha}\tau_{\pi/2}/\hbar} \langle e, n | \epsilon_{\beta} \rangle \langle \epsilon_{\beta} | j, k \rangle \langle j, k | \epsilon_{\alpha} \rangle \langle \epsilon_{\alpha} | g, n_0 \rangle \right|^2, \quad (24)$$

with $\epsilon_{j,n}$ being the bare energies corresponding to the $|j, n\rangle$ bare states ($j = g, e$), see Eq. (2). The excited state probability distribution will be given again by Eq. (4) in the general case, which is plotted in Fig. 5. It can be shown (Appendix C), that for weak lasers, the central maximum is shifted by

$$\delta(T) \approx \Omega_R \eta^2 \alpha^2 \left(\frac{2}{2 + \Omega_R T} \right) \left[\cos \frac{\omega_T T_t}{2} \sin \frac{\omega_T T}{2} + \alpha \left(\cos^2 \frac{\omega_T T_t}{2} + \sin^2 \frac{\omega_T T}{2} \right) \right], \quad (25)$$

which is also independent of the initial vibrational quantum number n_0 and where $T_t = 2\tau_{\pi/2} + T$ is the total time of the experiment, see Fig. 6. In the $T \rightarrow 0$ limit, this expression reduces to the one calculated for the Rabi case when a π -pulse is applied, see Eq. (18). For non-zero intermediate times T , the leading order in α in Eq. (25) may be written as

$$\delta(T) \approx \frac{2\Omega_R \eta^2 \alpha^2}{2 + \Omega_R T} \cos \frac{\omega_T T_t}{2} \sin \frac{\omega_T T}{2}, \quad (26)$$

with approximate upper and lower bounds given by

$$\delta(T) \approx \pm \frac{2\Omega_R \eta^2 \alpha^2}{2 + \Omega_R T}, \quad (27)$$

see again Fig. 6 (solid lines).

V. DISCUSSION

We have obtained analytical formulae that quantify the motional (sideband) effects in the carrier frequency peak of a trapped ion illuminated by a laser in the asymptotic Lamb-Dicke regime of tight confinement. Estimates of the importance of these effects for current or future experiments have been provided in Tables I and II. The importance of the shift discussed here depends greatly on the application and illumination scheme. Three different situations have been considered:

(a) In single pulse Rabi interferometry, long laser pulses are in principle desired in order to obtain narrow transitions, since the transition width is proportional to $1/\tau$, but this is limited by the stability of the laser and by the finite lifetime of the excited state. Typical laser pulses are of the order of milliseconds, that is, Rabi frequencies of tens to hundreds of Hertz if π -pulses (maximum excitation) are applied, which gives a frequency shift of 10^{-8} to 10^{-14} Hz, see Table I. Currently, the most

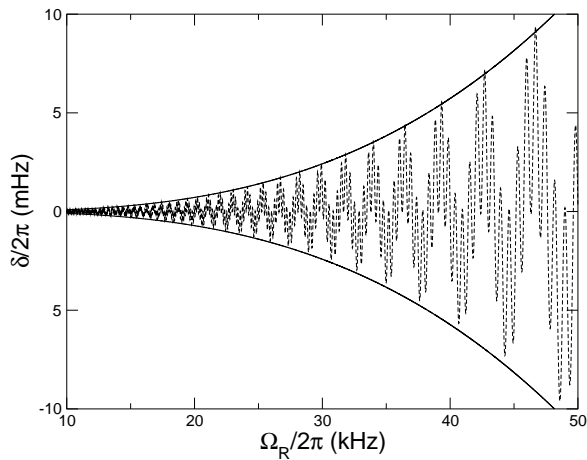


FIG. 6: Exact frequency shift (dashed line) and approximate upper and lower bounds (solid lines) as a function of the Rabi frequency after a Ramsey $\pi/2$ -pulse sequence with intermediate non-interaction time $T = 5\tau$. An ion trapped within the LD regime ($\eta = 0.04$) with a motional frequency $\omega_T = 2\pi \times 2\text{MHz}$ has been considered.

accurate absolute measurement of an optical frequency has fractional uncertainty of about 10^{-16} , but frequency standards based on an optical transition in a single stored ion have the potential to reach a fractional frequency uncertainty approaching 10^{-18} [11]. This means that the frequency shift found here corresponds to fractional errors of the order of $10^{-24} - 10^{-30}$ for typical optical transitions, which is far beyond the 10^{-18} level so that the shifts can be neglected in this context in the foreseeable future.

(b) This changes significantly for quantum information applications where fast operations are important and therefore the shifts are many orders of magnitude bigger even in the Rabi scheme, see Table II.

(c) Back to metrology, the shift in the Ramsey scheme is more significant than in the Rabi scheme, because the illumination times are much shorter and thus the Rabi frequencies are correspondingly higher. In recent Ramsey experiments with the $^{88}\text{Sr}^+$ ion at 674nm a trap with motional frequency $\omega_T \approx 2\pi \times 2\text{MHz}$ ($\eta \approx 0.042$) is driven by a laser with Rabi frequency $\Omega_R \approx 2\pi \times 16\text{kHz}$, which corresponds to laser pulses of several μs [16]. Different intermediate times T are used, ranging from $T = \tau$ to $T = 10\tau$. It is clear from Eq. (27) that the frequency shift decreases as the non interaction times T increases. With these data, Eq. (27) gives frequency shifts of $\delta \approx 2\pi \times 1\text{mHz}$ for $T = \tau$, which corresponds to a fractional error of order 10^{-18} . The effect is therefore small today, but relevant for the most accurate experiments in the near future.

Finally, a word is in order concerning the physical nature and interpretation of the shifts studied here. They are obviously associated with motional effects induced by the laser on the trapped ion, but they do not reflect en-

ergy level shifts. Our frequency shifts are defined by the carrier peak displacement of the excitation probability. This probability is calculated with a linear combination of dressed states, as in Eqs. (9) and (24). However, note that, while the eigenstates are affected (corrected) by the laser coupling of motional states characterized by the Lamb-Dicke parameter η , the energy eigenvalues remain unaffected in first order in η , see the Appendix A. Indeed, the exact calculations of the shift (based on the general Hamiltonian (1) and converged with respect to the number of levels) are reproduced by the approximations in which the eigenenergies remain unchanged, i.e., as in zeroth order with respect to η . The carrier peak shifts we have examined may in summary be viewed not as the result of energy-level shifts but due to dressed state corrections which affect the dynamics anyway. A consequence is their dependence on the illumination time.

Acknowledgements

This work has been supported by Ministerio de Educación y Ciencia (FIS2006-10268-C03-01) and UPV-EHU (00039.310-15968/2004).

APPENDIX A: PERTURBATIVE CORRECTIONS TO THE SEMIDRESSED STATES.

The semidressed Hamiltonian (11) is easily diagonalized, with semidressed (i.e., zeroth order) energies and states given by

$$\epsilon_{n,\pm}^{(0)} = E_n \pm \frac{\hbar\Omega}{2}, \quad (\text{A1})$$

$$|\epsilon_{n,\pm}^{(0)}\rangle = \frac{1}{\sqrt{N_{\pm}}} \left(\frac{\Delta \pm \Omega}{\Omega_R} |g, n\rangle + |e, n\rangle \right), \quad (\text{A2})$$

N_{\pm} being dimensionless normalization factors given by

$$N_{\pm} = \frac{(\Delta \pm \Omega)^2}{\Omega_R^2} + 1 = \frac{2\Omega}{\Omega_R^2} (\Omega \pm \Delta). \quad (\text{A3})$$

The dressed energies and states will be calculated by standard (time-independent) perturbation theory, with the perturbation given by the coupling term $V(\eta)$, see Eq. (11). The matrix elements connecting the semidressed states are given in the LD regime by [10]

$$\begin{aligned} & \langle \epsilon_{n,s}^{(0)} | V(\eta) | \epsilon_{n',s'}^{(0)} \rangle \\ &= i\eta s' \frac{\hbar\Omega}{\sqrt{N_s N_{s'}}} \left(\sqrt{n'} \delta_{n,n'-1} + \sqrt{n'+1} \delta_{n,n'+1} \right) (1 - \delta_{ss'}), \end{aligned}$$

where s and s' is a shorthand notation representing the sign ($s, s' = \pm$). Perturbation theory provides expressions for the dressed energies

$$\epsilon_{n,\pm} = \epsilon_{n,\pm}^{(0)} + \mathcal{O}(\eta^2) \quad (\text{A4})$$

with no linear corrections, since the diagonal terms of the matrix elements (A4) are zero. The dressed states (up to linear terms in η) are given by

$$|\epsilon_{n-1,\pm}\rangle = |\epsilon_{n-1,\pm}^{(0)}\rangle \pm \frac{i\eta\Omega_R\sqrt{n}}{-\omega_T \pm \Omega} |\epsilon_{n,\mp}^{(0)}\rangle, \quad (\text{A5})$$

$$\begin{aligned} |\epsilon_{n,\pm}\rangle &= |\epsilon_{n,\pm}^{(0)}\rangle \pm \frac{i\eta\Omega_R\sqrt{n}}{\omega_T \pm \Omega} |\epsilon_{n-1,\mp}^{(0)}\rangle \\ &\pm \frac{i\eta\Omega_R\sqrt{n+1}}{-\omega_T \pm \Omega} |\epsilon_{n+1,\mp}^{(0)}\rangle, \end{aligned} \quad (\text{A6})$$

$$|\epsilon_{n+1,\pm}\rangle = |\epsilon_{n+1,\pm}^{(0)}\rangle \pm \frac{i\eta\Omega_R\sqrt{n+1}}{\omega_T \pm \Omega} |\epsilon_{n,\mp}^{(0)}\rangle. \quad (\text{A7})$$

APPENDIX B: 4-STATE MODEL, EXACT SOLUTION

If the ion is previously cooled down to its ground $|g, 0\rangle$ state (e. g., via sideband cooling), the problem becomes 4-dimensional, since no red sideband will be involved, and analytical dressed states can be obtained without using the perturbative treatment of Section III A. In this 4-state model the excited state probability will then read

$$P_e \approx P_{e,0} + P_{e,1} \quad (\text{B1})$$

within the LD regime. The expressions for the dressed eigenenergies are given by

$$\epsilon_{s,s'} = \hbar\omega_T + s\frac{\hbar\nu_{s'}}{2}, \quad (\text{B2})$$

where s and s' is a shorthand notation representing a sign ($s, s' = \pm$). The (angular) frequencies ν_{\pm} are defined by $\nu_{\pm} \equiv \sqrt{(\omega_T \pm \Omega)^2 + \eta^2\Omega_R^2}$, with $\Omega \equiv \sqrt{\Omega_R^2 + \Delta^2}$ as usual. Near $\Delta = 0$, these ν_{\pm} are frequencies shifted to the blue and red with respect to the trap frequency ω_T ; they correspond to transitions among the dressed levels and play an important role in the carrier frequency shift as we shall see. The corresponding dressed eigenstates can be written as a function of the bare states,

$$\begin{aligned} |\epsilon_{s,s'}\rangle &= \frac{1}{\sqrt{N_{s,s'}}} \left[\frac{i}{\Omega_R} (\omega_T + s'\Omega - s\nu_{s'}) |g, 0\rangle \right. \\ &+ \frac{\eta\Omega_R}{s'\Omega - \Delta} |g, 1\rangle \\ &- \frac{i}{s'\Omega - \Delta} (\omega_T + s'\Omega - s\nu_{s'}) |e, 0\rangle \\ &\left. + \eta |e, 1\rangle \right], \end{aligned} \quad (\text{B3})$$

with $N_{s,s'}$ being normalization factors. (Strictly speaking, these states are ‘‘partially’’ dressed states in the sense that they are eigenstates of a part of the full Hamiltonian.)

If the ion is assumed initially in the ground $|g, 0\rangle$ state and is illuminated by a single laser pulse for a time τ ,

the probability of $|e, n\rangle$ is

$$P_{e,n} = \left| \sum_{s,s'} e^{-i\epsilon_{s,s'}\tau/\hbar} \langle e, n | \epsilon_{s,s'} \rangle \langle \epsilon_{s,s'} | g, 0 \rangle \right|^2, \quad (\text{B4})$$

which may be analytically calculated to give

$$\begin{aligned} P_{e0} &= \left(\frac{\Omega_R}{2\Omega} \right)^2 \left[\left(\cos \frac{\nu_+\tau}{2} - \cos \frac{\nu_-\tau}{2} \right)^2 \right. \\ &\left. + \left(\frac{\omega_T + \Omega}{\nu_+} \sin \frac{\nu_+\tau}{2} - \frac{\omega_T - \Omega}{\nu_-} \sin \frac{\nu_-\tau}{2} \right)^2 \right], \end{aligned} \quad (\text{B5})$$

$$\begin{aligned} P_{e1} &= \left(\frac{\eta\Omega_R}{2\Omega} \right)^2 \\ &\times \left(\frac{\Omega - \Delta}{\nu_+} \sin \frac{\nu_+\tau}{2} + \frac{\Omega + \Delta}{\nu_-} \sin \frac{\nu_-\tau}{2} \right)^2. \end{aligned} \quad (\text{B6})$$

These are ‘‘exact’’ results within the LD and four-level approximations. The oscillations in P_{e0} and P_{e1} may thus be viewed as interferences among the dressed states contributions and be characterized by frequencies ν_{\pm} .

Note also that the expressions (B5) and (B6) are valid for lasers of arbitrary intensity. In particular, transitions to higher order sidebands which in principle are off-resonant when $\Delta = 0$, become important when the ‘‘Rabi Resonance’’ condition $\Omega_R = \omega_T$ is fulfilled. In this case P_{e1} reduces to

$$P_{e1} \approx \frac{1}{4} \sin^2 \frac{\eta\Omega_R t}{2}. \quad (\text{B7})$$

which shows that terms which are in principle off-resonant lead to resonant effects under certain conditions, see also [10, 20, 21, 22, 23].

Expressions (B5) and (B6) can be further simplified by performing an expansion in power series of the LD parameter. To leading order in η ,

$$\begin{aligned} P_{e0} &\approx \left(\frac{\Omega_R}{\Omega} \right)^2 \sin^2 \frac{\Omega t}{2} \left[1 - \left(\frac{\Omega t}{2} \right) \frac{\eta^2\Omega_R^2}{\omega_T^2} \cot \frac{\Omega t}{2} \right], \\ P_{e1} &\approx \left(\frac{\eta\Omega_R}{2\Omega} \right)^2 \left[A_+ \sin \frac{(\omega_T + \Omega)t}{2} + A_- \sin \frac{(\omega_T - \Omega)t}{2} \right]^2, \end{aligned}$$

with $A_{\pm} = \frac{\Omega \mp \Delta}{\omega_T \pm \Omega}$. $P_{e1}(t)$ takes the form of a beating oscillation with a fast frequency ω_T and a slow frequency Ω_R .

The expressions for the excited state probability simplify when the duration of the laser pulse is fixed. If a π -pulse is applied ($\tau = \pi/\Omega_R$) we have that

$$P_{e0} \approx \left(\frac{\Omega_R}{\Omega} \right)^2, \quad (\text{B8})$$

$$P_{e1} \approx \left(\frac{\eta\Omega_R}{2\Omega} \right)^2 (A_+ - A_-)^2 \cos^2 \frac{\omega_T \tau \pi}{2}, \quad (\text{B9})$$

which, near atomic resonance ($\Delta \sim 0$), can be written as

$$P_{e0} \approx 1 - \frac{\Delta^2}{\Omega_R^2}, \quad (\text{B10})$$

$$P_{e1} \approx \eta^2 \left(\frac{\Omega_R^4}{\omega_T^4} + \frac{2\Omega_R^2\Delta}{\omega_T^3} + \frac{\Delta^2}{\omega_T^2} \right) \cos^2 \frac{\omega_T \tau_\pi}{2}. \quad (\text{B11})$$

With these expressions for the excited state probabilities, the shifted position of the central resonance follows from Eq. (7): the central maximum in Fig. 1 is pulled to the right, to higher frequencies, by

$$\delta(\tau_\pi) \approx \Omega_R \eta^2 \alpha^3 \cos^2 \frac{\omega_T \tau_\pi}{2}, \quad (\text{B12})$$

the same result obtained in the general 6-state model calculation when a π -pulse is applied, see Eq. (18).

APPENDIX C: DERIVATION OF THE FREQUENCY SHIFT IN THE RAMSEY CASE

From Eq. (24) and with the (approximate) dressed energies (A4) and dressed states (A5) obtained in Appendix A, we may calculate the probabilities for the different $|e, n\rangle$ states. To leading order in the LD parameter and near atomic resonance $\Delta \sim 0$, they are given by

$$\begin{aligned} P_{e, n_0 \pm 1} &\approx \frac{N\eta^2}{(1-\alpha^2)^2} \left[\left(\alpha^2 \cos \frac{\omega_T T_t}{2} + \alpha \sin \frac{\omega_T T}{2} \right)^2 \right. \\ &\quad \pm \frac{\alpha\Delta}{\omega_T} (2 + T\Omega_R) \left(\cos \frac{\omega_T T_t}{2} + \alpha \sin \frac{\omega_T T}{2} \right) \\ &\quad \left. \times \left(\alpha \cos \frac{\omega_T T_t}{2} + \sin \frac{\omega_T T}{2} \right) \right], \\ P_{e, n_0} &\approx 1 - \left(\frac{1}{\Omega_R^2} + \frac{T}{\Omega_R} + \frac{T^2}{4} \right) \Delta^2, \end{aligned} \quad (\text{C1})$$

with $N = n_0$ ($N = n_0 + 1$) for the red (blue) sideband. The presence of the blue and red sidebands will shift the position of the central resonance to a position satisfying the maximum condition (7). This gives a shift of

$$\begin{aligned} \delta(T) &\approx \Omega_R \eta^2 \frac{\alpha^2}{(1-\alpha^2)^2} \left(\frac{2}{2 + T\Omega_R} \right) \\ &\quad \times \left(\cos \frac{\omega_T T_t}{2} + \alpha \sin \frac{\omega_T T}{2} \right) \left(\alpha \cos \frac{\omega_T T_t}{2} + \sin \frac{\omega_T T}{2} \right). \end{aligned}$$

Keeping leading order terms in α if low intensity lasers are assumed ($\alpha = \Omega_R/\omega_T \ll 1$) gives the frequency shift

$$\begin{aligned} \delta(T) &\approx \Omega_R \eta^2 \alpha^2 \left(\frac{2}{2 + \Omega_R T} \right) \left[\cos \frac{\omega_T T_t}{2} \sin \frac{\omega_T T}{2} \right. \\ &\quad \left. + \alpha \left(\cos^2 \frac{\omega_T T_t}{2} + \sin^2 \frac{\omega_T T}{2} \right) \right], \end{aligned} \quad (\text{C2})$$

which is Eq. (25).

-
- [1] D. Leibfried, R. Blatt, C. Monroe, and D. Wineland, *Rev. Mod. Phys.* **75**, 281 (2003).
[2] D. J. Wineland, C. Monroe, W. M. Itano, D. Leibfried, B. E. King, and D. M. Mekhof, *J. Res. Natl. Inst. Stand. Technol.* **103**, 259 (1998).
[3] D. J. Wineland, W. M. Itano, *Phys. Rev. A* **20**, 1521 (1975).
[4] R. H. Dicke, *Phys. Rev.* **89**, 472 (1952).
[5] A.A. Madej and J.E. Bernard, "Single Ion Optical Frequency Standards and Measurement of their Absolute Optical Frequency", in: *Frequency Measurement and Control : Advanced Techniques and Future Trends*, Springer Topics in Applied Physics, Andre N. Luiten editor, vol .79, (Springer Verlag, Berlin, Heidelberg, 2001) p. 153-194.
[6] H. Häffner *et al.*, *Phys. Rev. Lett.* **90**, 143602 (2003).
[7] F. Schmidt-Kaler *et al.*, *Europhys. Lett.* **65**, 587 (2004).
[8] J. Eschner *et al.*, *J. Opt. Soc. Am. B* **20**, 1003 (2003).
[9] J. I. Cirac, R. Blatt, P. Zoller, *Phys. Rev. A* **49**, R3174 (1994).
[10] I. Lizuain, J. G. Muga, *Phys. Rev. A* **75**, 033613 (2007).
[11] W. H. Oskay *et al.*, *Phys. Rev. Lett.* **97**, 020801 (2006).
[12] S. A. Diddams *et al.*, *Science* **293**, 825 (2001).
[13] C. Champenois *et al.*, *Phys. Lett. A* **331** 298-311 (2004).
[14] E. Riis and A. G. Sinclair, *J. Phys. B: At. Mol. Opt. Phys* **37** 4719-4732 (2004).
[15] Th. Udem *et al.* *Phys. Rev. Lett.* **86** 4996 (2001).
[16] V. Letchumanan, P. Gill, E. Riis, and A. G. Sinclair, *Phys. Rev. A* **70**, 033419 (2004).
[17] J. I. Cirac and P. Zoller, *Phys. Rev. Lett.* **74**, 4091 (1995).
[18] F. Schmidt-Kaler *et al.* *Nature* **74**, Issue 6930, pp. 408-411 (2003)
[19] N. F. Ramsey, *Phys. Rev.* **78**, 695 (1950).
[20] I. Lizuain, J. G. Muga, *Phys. Rev. A* **74**, 053608 (2006).
[21] D. Jonathan, M. B. Plenio, and P. L. Knight, *Phys. Rev. A* **62**, 042307 (2000).
[22] H. Moya-Cessa, A. Vidiella-Barranco, J. A. Roversi, D. S. Freitas, and S. M. Dutra, *Phys. Rev. A* **59**, 2518 (1999).

- [23] P. Aniello, A. Porzio and S. Solimeno, *J. Opt. B: Quantum Semiclass. Opt.* **5**, S233 (2003).